Reconstruction of Multi-Dimensional Bandlimited Signals from Nonuniform and Generalized Samples.

A. Feuer*
Department of Electrical Engineering, Technion, Haifa 32000, Israel
email: feuer@ee.technion.ac.il, http://www.ee.technion.ac.il

G. C. Goodwin
School of Electrical Eng. & Computer Sci.,
University of Newcastle, Newcastle, Australia

Abstract – This paper addresses the problem of multi-dimensional signal reconstruction from nonuniform or generalized samples. Typical solutions in the literature for this problem, utilize continuous filtering. The key result of the current paper is a multi-dimensional "interpolation" identity which establishes the equivalence of two multi-dimensional processing operations. One of these uses continuous domain filters while the other uses discrete processing. This result has obvious benefits in the context of the afore mentioned problem. The results here expand and generalize earlier work by other authors on the one dimensional case. Potential applications include 2D images and video signals

Keywords: Multi-dimensional sampling, nonuniform sampling, reconstruction

EDICS: 2–RECO

* **Corresponding Author**

1 Introduction

Discrete multi-dimensional signal processing inherently relies on sampling a continuous multi-variable signal. In this way, a multi-dimensional discrete representation of the signal is obtained. By a multi-dimensional signal we mean a signal which depends on more than one variable. (Examples include 2D images and 3D video). The most common form of sampling is on a lattice which is the multi-dimensional equivalent of uniform sampling in the one dimensional case. (A brief overview of lattices will be provided in the next section.) In many applications, however, the data inherently has a more complex structure. For example, it might be generated by non-uniform sampling or by sampling multi-channel versions of the original signals.

Two specific applications which have motivated the author's interest in the questions addressed in the current paper are (i) resolution enhancement of fiberoptic endoscopes and (ii) resolution enhancement and video compression in digital video cameras. In the first of these applications, the fiberoptic size and the endoscope diameter put a constraint on possible image resolution as each fiber transfers a single pixel of the image. In this project we generate multiple images with temporal changes and use them to generate a single image of improved resolution. In the second application, one uses multiple video cameras to capture different aspects of the same scene. Some may emphasize spatial resolution whilst others may emphasize temporal resolution, i.e., frame rate. The problem is then to use the multiple clips to gain a single video clip with enhanced resolution, both spatial and temporal. The problem is made more difficult because each camera will have a different sampling pattern. Some details of these applications are commercially sensitive at this stage but the basic technical issues involved are addressed in the two specific patterns analyzed in Sections 4 and 5 of this paper.

Reconstruction of signals from *uniform* sampling (i.e. on a lattice) is a straightforward generalization of the one dimensional case using lowpass filters, (see e.g. [9], [2], [14]). However, existing methods for reconstruction from other types of data, such as those mentioned above, typically use continuous filters (see e.g.[1] and [3]) and are thus unsuitable for digital implementation.

In [4] the authors address the above issues for the one dimensional case. Specifically, they introduce a result coined the 'Interpolation Identity'. This identity is shown to lead to efficient reconstruction methods from generalized samples as well as efficient interpolation to uniformly spaced samples.

In the current paper we generalize the results presented in [4] to multi-dimensional signals. Potential applications of the results described here would include:

- Taking digital photographs of the same scene using identical or different digital cameras
- Analyzing video images of the same scene taken by different cameras.

The resultant identity is, in fact, a statement of equivalence between two configurations to process sampled data signals having a continuous signal as output. In one of the

configurations, the processing is done in the continuous domain using continuous filters. In the alternative configuration, the processing is done in the discrete domain. A key property of the second configuration is that it leads to a discrete representation having "uniform" samples (i.e. sampled on a lattice). If required, the continuous signal can be recovered form these "uniform samples" via a multivariable lowpass filtering operation [2]. However, in other cases, the conversion to uniform samples (on a lattice) could be a desirable end-point in its own right.

The layout of the remainder of the paper is as follows. In Section 2 we provide a brief overview of multi-dimensional sampling and introduce the notation to be used in the sequel. In Section 3, we state and prove the key result of this paper, namely, a multi-dimensional version of the 'Interpolation identity' introduced in [4] for the 1D case. This involves several novel aspects which are not present in the one dimensional case. Section 4 and Section 5 consider two cases of multi-dimensional recurrent sampling based on the Generalized Sampling Expansion (GSE) (see e.g. [1] and [6]). For these cases, the multi-dimensioanl Interpolation Identity is applied to generate an efficient implementation algorithm.

2 Background to multi-dimensional sampling

2.1 Sampling Lattices and Noncommutative Rings

The generalization of the concept of uniform sampling in the one dimensional case to multivariable sampling leads to the notion of a 'sampling lattice' (see e.g. [2]). By a sampling *lattice* we refer to a set:

$$\mathcal{LAT}\left(T\right)=\left\{T\underline{n}:\underline{n}\in\mathbb{Z}^{D}\right\}\subset\mathbb{R}^{D} \tag{1}$$

for a given nonsingular matrix $T\in\mathbb{R}^{D\times D}$. Here we have used $\mathbb{Z}$, $\mathbb{R}$ to denote the integers and reals respectively. The generalization of a 'sampling interval' in the 1D case to the multi-dimensional case leads to the concept of a *unit cell*. A unit cell $\mathcal{UC}\left(T\right)\subset\mathbb{R}^{D}$ associated with the sampling lattice $\mathcal{LAT}\left(T\right)$, is a set with the following two properties: $\left\{\mathcal{UC}\left(T\right)+T\underline{n}_{1}\right\}\cap\left\{\mathcal{UC}\left(T\right)+T\underline{n}_{2}\right\}=\varnothing$ for any $\underline{n}_{1},\underline{n}_{2}\in\mathbb{Z}^{D}$, $\underline{n}_{1}\neq\underline{n}_{2}$ and $\bigcup_{\underline{n}\in\mathbb{Z}^{D}}\left\{\mathcal{UC}\left(T\right)+\underline{n}\right\}=\mathbb{R}^{D}$. A given lattice gives rise to many unit cells. However, all possible unit cells of the same lattice have an identical volume given by $\left|\det\left(T\right)\right|$. A *set of representatives* of a given lattice over the integers, $\mathcal{LAT}\left(K\right)$, where K is an integer matrix, is defined to be the set

$$\mathcal{SR}\left(K\right)=\mathcal{UC}\left(K\right)\cap\mathcal{LAT}\left(I\right) \tag{2}$$

where I is the identity matrix (hence $\mathcal{LAT}\left(I\right)=\mathbb{Z}^{D}$). Clearly, since the unit cell is not unique, neither is $\mathcal{SR}\left(K\right)$. However, it can be shown (see [8]) that the number of elements in every $\mathcal{SR}\left(K\right)$ is the same and is equal to $\left|\det\left(K\right)\right|$.

Important insights into sampling lattices are also provided from their equivalent frequency domain representations. In this context one can either use normalized frequencies (as is often done in the signal processing literature) or un-normalized frequencies (as

discussed in detail in [7]). Both are equivalent and thus it is a matter of taste as to which one decides to use for a given problem. In this paper, we will use un-normalized frequencies since by doing so we maintain the same scale of the frequency domain operator which allows easier comparison of the effect of different sampling patterns.

Using these ideas, then for every sampling lattice $\mathcal{LAT}(T)$, there exists a *polar* (or *reciprocal*) lattice defined by $\mathcal{LAT}\left(2\pi T^{-T}\right)$ with the property that $\underline{\omega}^T\underline{x}$ is an integer multiple of 2π for every $\underline{\omega} \in \mathcal{LAT}\left(2\pi T^{-T}\right)$, $\underline{x} \in \mathcal{LAT}(T)$. The reciprocal lattice plays a key role for signals sampled on $\mathcal{LAT}(T)$. In particular, it represents the frequency domain effect of sampling on $\mathcal{LAT}(T)$. This is analogous to the relationship between $\{n\Delta t\}$ and $\left\{k\frac{2\pi}{\Delta t}\right\}$ in the one dimensional case.

The above points highlight the core difference between the one dimensional and multi-dimensional cases. Specifically, in the one dimensional case we need to deal with integers (i.e., a *commutative ring*), whilst, in the multi-dimensional case, we will need to deal with square matrices of integers (i.e., a *non-commutative ring*). This key difference leads to major difficulties in the multi-dimensional case, both in terms of the formulation and derivation of results. One aspect of this difficulty is highlighted in [15] where it is pointed out that the lack of commutativity prevents decimators and expanders to be commuted in the multidimensional case (see also [10] or [5]). This particular issue was later resolved in [8]. This reference also introduces various tools which we will make use of and generalize in the sequel.

For completeness, we summarize below some facts regarding non-commutative rings which we will utilize. We refer the reader to [11], [12], [15] and, in particular [8] for further details.

Given three matrices $M, M_o, S \in \mathbb{Z}^{D\times D}$ which satisfy $M = SM_o$, we call S a *left devisor* of M. M is called a *left multiple* of M_o. A *greatest common left (right) divisor,* g.c.l.d (g.c.r.d) $S \in \mathbb{Z}^{D\times D}$ of two matrices $M, R \in \mathbb{Z}^{D\times D}$ is a common left (right) divisor which is a right (left) multiple of every common left (right) devisor of M and R. $S \in \mathbb{Z}^{D\times D}$ is said to be unimodular if $|\det(S)| = 1$. M and R are *left (right) coprime* if their g.c.l.d (g.c.r.d) is unimodular. It is known that (see e.g. [8]) , for every left coprime nonsingular M_o and R_o, there exists right coprime pairs $\widetilde{M}_o, \widetilde{R}_o \in \mathbb{Z}^{D\times D}$ such that $M_o^{-1}R_o = \widetilde{R}_o\widetilde{M}_o^{-1}$with $|\det(M_o)| = \left|\det\left(\widetilde{M}_o\right)\right|$. Hence, one can readily observe that for any nonsingular integral M, R there exist a pair $\widetilde{M}$, $\widetilde{R}$ for which

$$\begin{aligned} M^{-1}R &= \widetilde{R}\widetilde{M}^{-1} \\ |\det(M)| &= \left|\det\left(\widetilde{M}\right)\right| \end{aligned} \tag{3}$$

We illustrate the last point by the following simple example (This example will be utilized in the sequel to further illustrate multi-dimensional sampling ideas and concepts):

Example 1 Let

$$M = \begin{bmatrix} 2 & 1 \\ 0 & 2 \end{bmatrix}; R = \begin{bmatrix} 1 & 0 \\ 1 & 3 \end{bmatrix} \tag{4}$$

Then we can choose

$$\widetilde{M} = \begin{bmatrix} 4 & -3 \\ 0 & -1 \end{bmatrix}; \widetilde{R} = \begin{bmatrix} 1 & 0 \\ 2 & -3 \end{bmatrix} \tag{5}$$

and properties (3) can readily be verified.

■

2.2 Preliminary Results

We assume that the continuous signals, which we denote $f_c(\underline{x}), \underline{x} \in \mathbb{R}^D$, are bandlimited in the sense that there exists a sampling lattice $\mathcal{LAT}(T_Q)$ with the property that

$$\text{support}\left(\widehat{f_c}(\underline{\omega})\right) \subseteq \mathcal{UC}\left(2\pi T_Q^{-T}\right) \tag{6}$$

Here, and elsewhere, we use $\hat{\gamma}(\underline{\omega})$ to denote the multi-dimensional Fourier Transform of the signal $\gamma(\underline{x})$.

The lattice $\mathcal{LAT}(T_Q)$ can be viewed as the multivariable generalization of the "Nyquist rate" in the one dimensional case. For this reason, we call it a "Nyquist lattice".

Clearly, the signal $f_c(\underline{x})$ could be reconstructed from its sampled values on $\mathcal{LAT}(T_Q)$ by passing $f_d(\underline{x}) = \sum_{\underline{n}\in\mathbb{Z}^D} f_c(T_Q\underline{n})\,\delta(\underline{x} - T_Q\underline{n})$ through the ideal lowpass filter

$$\widehat{h}_{LP}(\underline{\omega}) = \begin{cases} |\det(T_Q)| & \text{for } \underline{\omega} \in \mathcal{UC}\left(2\pi T_Q^{-T}\right) \\ 0 & \text{otherwise} \end{cases} \tag{7}$$

However, our interest here is in generalized sampling. Thus, we assume that the actual sampling lattice we employ is $\mathcal{LAT}(T)$. We impose the following constraint on the relationship between $\mathcal{LAT}(T)$ and $\mathcal{LAT}(T_Q)$:

Assumption 1 : T and T_Q are related via

$$\begin{aligned} T &= T_Q M^{-1} R \\ &= T_Q \widetilde{R}\widetilde{M}^{-1} \end{aligned} \tag{8}$$

where $R, M, \widetilde{R}, \widetilde{M} \in \mathbb{Z}^{D\times D}$ are non singular matrices satisfying (3).

■

Note that Assumption 1 is not very restrictive. Indeed, in the scalar case, it simply reduces to the fact that the ratio $\frac{T}{T_Q}$ is rational. In the multivariable case, a sufficient condition is that the entries in T and T_Q are rational.

Assumption 1 (equation (8)), guarantees that $\mathcal{LAT}(T_Q)$ (the Nyquist lattice) can be generated from $\mathcal{LAT}(T)$ through expansion of $\mathcal{LAT}(T)$ by a factor of R and then

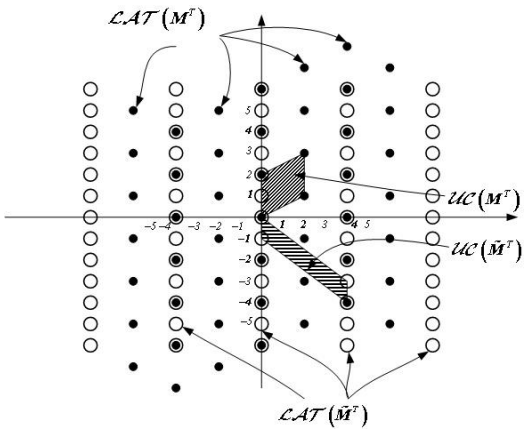

Figure 1: The lattices$\mathcal{LAT}\left(M^T\right)$ and $\mathcal{LAT}\left(\widetilde{M}^T\right)$and their respective unit cells for the example.

decimation by a factor of M. These operations, for the multi-dimensional case, are discussed and demonstrated in Section 2.3 (see also [15]).

Let $M, \widetilde{M} \in \mathbb{Z}^{D\times D}$ be as in (3). We next consider the lattices $\mathcal{LAT}\left(M^T\right)$, $\mathcal{LAT}\left(\widetilde{M}^T\right)$, together with any of their respective unit cells $\mathcal{UC}\left(M^T\right)$, $\mathcal{UC}\left(\widetilde{M}^T\right)$ and their sets of representatives $\mathcal{SR}\left(M^T\right)$ and $\mathcal{SR}\left(\widetilde{M}^T\right)$. Clearly, since $\left|\det\left(M^T\right)\right| = \left|\det\left(\widetilde{M}^T\right)\right|$, the two sets of representatives contain the same number of distinct vectors, N. These observations are illustrated below:

Example 1 (continued). The above concepts are illustrated in Figure 1 for the example matrices given in (4) and (5). For the unit cells in Figure 1 we have $N = \left|\det\left(M^T\right)\right| = 4$. In particular, $\mathcal{SR}\left(M^T\right) = \left\{\begin{bmatrix}0\\0\end{bmatrix}, \begin{bmatrix}0\\1\end{bmatrix}, \begin{bmatrix}1\\1\end{bmatrix}, \begin{bmatrix}1\\2\end{bmatrix}\right\}$ and $\mathcal{SR}\left(\widetilde{M}^T\right) = \left\{\begin{bmatrix}0\\0\end{bmatrix}, \begin{bmatrix}1\\-1\end{bmatrix}, \begin{bmatrix}2\\-2\end{bmatrix}, \begin{bmatrix}3\\-3\end{bmatrix}\right\}$.

■

Note that by definition, for every $\underline{m} \in \mathbb{Z}^D$ there exist unique $\underline{n}, \widetilde{\underline{n}} \in \mathbb{Z}^D$ and $\underline{k} \in \mathcal{SR}\left(M^T\right), \widetilde{\underline{k}} \in \mathcal{SR}\left(\widetilde{M}^T\right)$ such that $\underline{m} = M^T\underline{n} + \underline{k} = \widetilde{M}^T\widetilde{\underline{n}} + \widetilde{\underline{k}}$ (see [15]). We can then write $\underline{m} \equiv \underline{k} \bmod \left(M^T\right)$ and $\underline{m} \equiv \widetilde{\underline{k}} \bmod \left(\widetilde{M}^T\right)$. We thus have the following result which gives an explicit enumeration of $\mathcal{SR}\left(M^T\right)$ and $\mathcal{SR}\left(\widetilde{M}^T\right)$.

Lemma 1 The mapping $\rho : \mathcal{SR}\left(M^T\right) \to \mathcal{SR}\left(\widetilde{M}^T\right)$ defined by

$$\begin{aligned}\rho\left(\underline{k}\right) &\equiv \left(\widetilde{R}^T\underline{k}\right) \bmod \left(\widetilde{M}^T\right) \\ &= \widetilde{R}^T\underline{k} - \widetilde{M}^T\underline{n}\end{aligned} \tag{9}$$

is one to one and onto.

Proof. (See Appendix A). ■

We illustrate by continuing the example:

Example 1 (continued).

For the matrices in the example, we apply ρ as introduced in Lemma 1 and obtain:

$$\rho\left\{\begin{bmatrix}0\\0\end{bmatrix},\begin{bmatrix}0\\1\end{bmatrix},\begin{bmatrix}1\\1\end{bmatrix},\begin{bmatrix}1\\2\end{bmatrix}\right\} = \left\{\begin{bmatrix}0\\0\end{bmatrix},\begin{bmatrix}2\\-2\end{bmatrix}\begin{bmatrix}3\\-3\end{bmatrix},\begin{bmatrix}1\\-1\end{bmatrix},\right\}.$$

■

An immediate consequence of Lemma 1 is that we can enumerate the vectors $\underline{k}_1, ..., \underline{k}_N$ in $\mathcal{SR}\left(M^T\right)$ and $\widetilde{\underline{k}}_1, ..., \widetilde{\underline{k}}_N$ in$\mathcal{SR}\left(\widetilde{M}^T\right)$ such that

$$\widetilde{\underline{k}}_\ell = \rho\left(\underline{k}_\ell\right) \text{ for } \ell = 1, 2, ..., N \tag{10}$$

In the analysis presented below, in order to simplify notation, we describe discrete signals as weighted sums of Dirac Delta functions. This enables us to view them as continuous signals and eliminates the need to distinguish between continuous and discrete (normalized) frequencies. Hence, *we only use continuous frequencies* $\underline{\omega} \in \mathbb{R}^D$. The same holds for the filters we use - i.e. a discrete filter will have an impulse response which is a weighted sum of Dirac Delta functions and a frequency response which is *periodic* over the corresponding reciprocal lattice.

2.3 Multivariable Upsampling and Downsampling

In our development presented later, we will utilize expanding by a matrix factor R (multivariable upsampling) and decimating by a matrix factor M (multivariable downsampling) - both R and M are matrices of integers. In essence, these operations are similar to those used in the scalar case, however, the technical details can be significantly more intricate. Say, the initial sampling lattice is $\mathcal{LAT}\left(T\right)$. When expanded by R we get the lattice $\mathcal{LAT}\left(TR^{-1}\right) \supseteq \mathcal{LAT}\left(T\right)$ and when decimated by M we get the lattice $\mathcal{LAT}\left(TR^{-1}M\right) = \mathcal{LAT}\left(T_Q\right) \subseteq \mathcal{LAT}\left(TR^{-1}\right)$. As a demonstration we refer the reader to Figure 2 where we chose

$$T = \begin{bmatrix}\frac{1}{4} & -\frac{3}{4}\\ \frac{1}{2} & \frac{3}{2}\end{bmatrix}$$

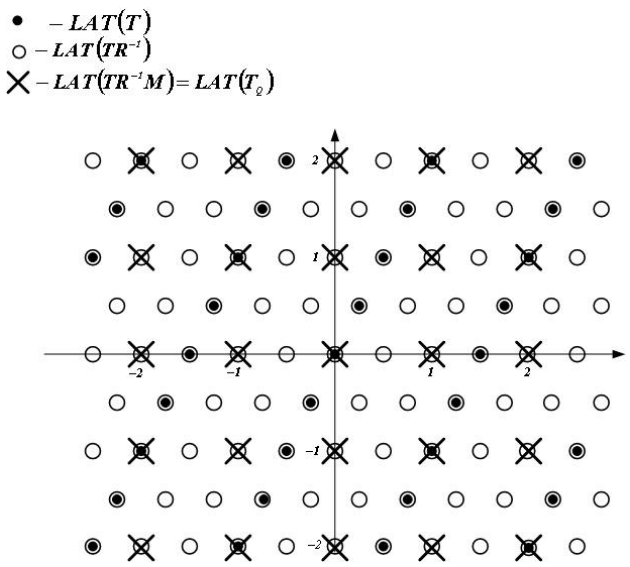

Figure 2: The input lattice $\mathcal{LAT}\left(T\right)$, expanded by R to give $\mathcal{LAT}\left(TR^{-1}\right)$ and decimated by M to give $\mathcal{LAT}\left(TR^{-1}M\right)$.

We also choose T_Q as the 2×2 - identity matrix and R, M as in the example - one can readily verify that Assumption 1 holds for these choices. The initial lattice $\mathcal{LAT}\left(T\right)$, is presented in Figure 2 by solid circles, the empty circles are $\mathcal{LAT}\left(TR^{-1}\right)$ and '$\times$' denotes $\mathcal{LAT}\left(TR^{-1}M\right)$. We see from the figure the relationships $\mathcal{LAT}\left(T\right) \subseteq \mathcal{LAT}\left(TR^{-1}\right)$ and $\mathcal{LAT}\left(TR^{-1}M\right) \subseteq \mathcal{LAT}\left(TR^{-1}\right)$. For a more detailed exposition on this subject the reader is referred to [15].

3 The Key Technical Result

In this section we state and prove our key result which is a multivariable interpolation identity. This establishes an equivalence between a continuous multivariable filter bank and a discrete filtering scheme involving upsampling and downsampling. The result extends a published result ([4]) for the 1D case to the multi-dimensional case. The two configurations are illustrated in Figures 3 and 4 respectively. These figures have been introduced so that the reader can better visualize the result. Both configurations are driven by the multivariable sampled data of $f_c\left(\underline{x}\right), \underline{x} \in \mathbb{R}^D$ sampled on $\mathcal{LAT}\left(T\right)$. However, the processing in Figure 3 is all in the continuous domain while in Figure 4 most of the processing is done in the discrete domain. Only the last step in Figure 4, a standard low pass filter (as given in (7)) which allows reconstruction from data sampled on a lattice, is continuous. The set up described in Figure 3 is motivated by the most general reconstruction problem we treat, namely the Pth order nonuniform sampling. We present this problem and illustrate the utility of our result in Section 5.

We further wish to point out that the filters $\{h_\ell\left(\underline{x}\right)\}_{\ell=1}^{N}$ in Figure (3) are bandlimited to $\mathcal{UC}\left(2\pi T_Q^{-T}\right)$ (which is also the bandwidth of the signal $f_c\left(\underline{x}\right)$). The signals $f\left(\underline{x}\right), f_e\left(\underline{x}\right), y_e\left(\underline{x}\right)$ and $y_d\left(\underline{x}\right)$ in Figure 4 are all discrete signals (i.e., sequences). The

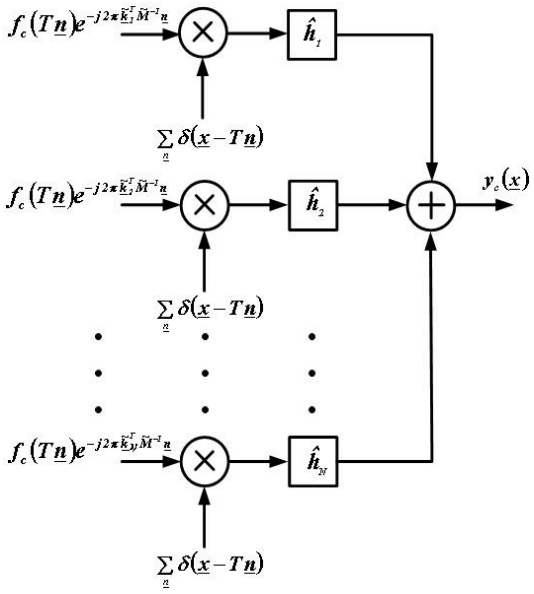

Figure 3: Continuous filter bank configuration.

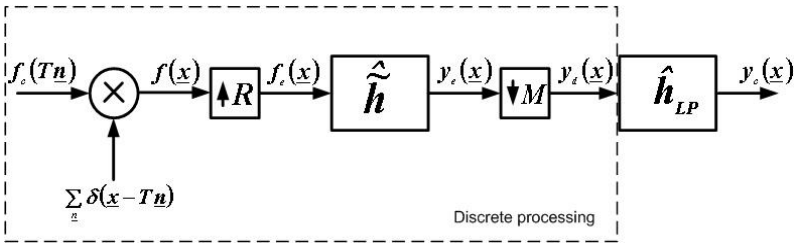

Figure 4: Equivalent discrete configuration.

same is true for the filter $\widetilde{h}(\underline{x})$ which is denoted by its frequency response $\widehat{\widetilde{h}}(\underline{\omega})$ in Figure 4. Note that $\widehat{\widetilde{h}}(\underline{\omega})$ is periodic, since it represents discrete processing (hence, its impulse response is a weighted sum of Dirac Delta functions). Also note that the signal $f_e(\underline{x})$ is the result of expanding $f(\underline{x})$ by a factor R and $y_d(\underline{x})$ results from decimating $y_e(\underline{x})$ by a factor M where both R and M are (integral) matrices.

Given the above background, we are now in a position to state and prove the following:

Theorem 1 *Let $f_c(\underline{x})$ be such that (6) is satisfied. Consider T, T_Q, satisfying Assumption 1, with M, R, $\widetilde{M}$, $\widetilde{R}$ as in (8) and $\{\underline{k}_\ell\}_{\ell=1}^N = \mathcal{SR}(M^T)$ $\left\{\widetilde{\underline{k}}_\ell\right\}_{\ell=1}^N = \mathcal{SR}\left(\widetilde{M}^T\right)$ enumerated so that (10) holds. Then, the configurations in Figures 3 and 4 are equivalent provided we choose*

$$\widehat{\widetilde{h}}(\underline{\omega}) = \frac{N}{|\det(T_Q)|} \sum_{\underline{n}\in\mathbb{Z}^D} \sum_{\ell=1}^{N} \widehat{h}_\ell\left(\underline{\omega} - 2\pi T_Q^{-T}\underline{k}_\ell + 2\pi T_Q^{-T} M^T \underline{n}\right) \tag{11}$$

Proof. (See Appendix B.) ■

Remark 1 *For the scalar case Assumption 1 becomes $T/T_Q = R/M$ for any coprime integers M, R. This generalizes the result in [4] where it is assumed that $T/T_Q - 1/M$ is an integer (namely, $R \equiv 1 \bmod (M)$).*

Remark 2 *Note that by virtue of (11), the resultant filter $\widehat{\widetilde{h}}(\omega)$ is indeed periodic in the expanded reciprocal lattice $\mathcal{LAT}\left(2\pi T^{-T}R^T\right) = \mathcal{LAT}\left(2\pi T_Q^{-T}M^T\right)$ i.e., $\widehat{\widetilde{h}}\left(\underline{\omega} + 2\pi T_Q^{-T}M^T\underline{n}\right) = \widehat{\widetilde{h}}(\underline{\omega})$ for all $\underline{\omega}$. Furthermore, equation (11) can be thought of as a tiling process over one "period" in the frequency domain i.e., over a unit cell of $\mathcal{LAT}\left(2\pi T^{-T}R^T\right)$. This unit cell is divided into $N = |\det(M)|$ unit cells of the reciprocal "Nyquist" lattice $\mathcal{LAT}\left(2\pi T_Q^{-T}\right)$. In each of the unit cells we place the shifted frequency response of one continuous filter. This process is illustrated in Figure 5 for the simple example above. In this figure we demonstrate how the unit cell $\mathcal{UC}\left(2\pi T^{-T}R^T\right)$ of the lattice $\mathcal{LAT}\left(2\pi T^{-T}R^T\right)$ (which is the period of filter $\widehat{\widetilde{h}}(\omega)$) is constructed from the unit cell of the 'Nyquist lattice' $\mathcal{LAT}\left(2\pi T_Q^{-T}\right)$ shifted by $2\pi T_Q^{-T}\underline{k}_\ell$ and how each period of $\widehat{\widetilde{h}}(\omega)$ is constructed from the filters $\widehat{h}_\ell(\omega)$ shifted by $2\pi T_Q^{-T}\underline{k}_\ell$ respectively.*

As an illustration of the utility of the above result we apply it, in the following sections, to some special cases namely, the reconstruction of a signal sampled on recurrent sampling patterns.

4 Multi-dimensional recurrent nonuniform sampling.

In this section, we consider a special case of multi-dimensional nonuniform sampling. Let $\mathcal{LAT}(T_Q)$ and $\mathcal{LAT}(T)$ be two sampling lattices. Assume that

$$T = T_Q R \tag{12}$$

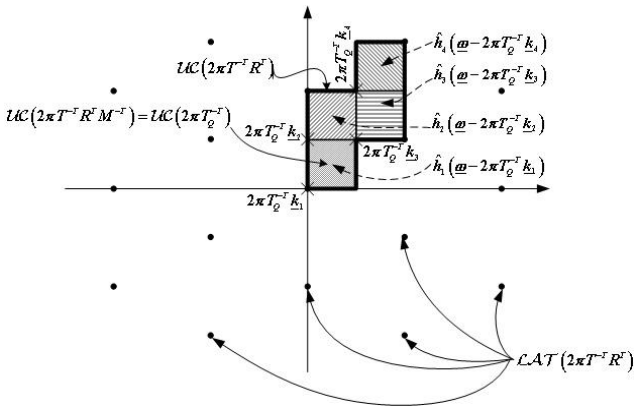

Figure 5: Demonstration of the 'tiling' construction of $\widehat{\widetilde{h}}(\underline{\omega})$ as defined in equation (11).

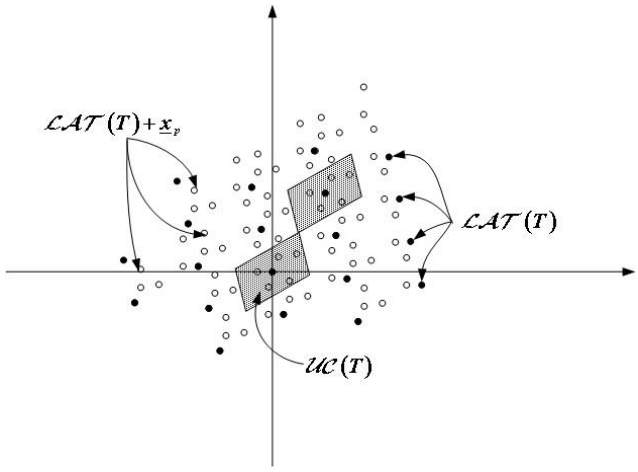

Figure 6: A 2D example of recurrent sampling.

for some nonsingular $R \in \mathbb{Z}^{D\times D}$. Thus, clearly $\mathcal{LAT}(T) \subset \mathcal{LAT}(T_Q)$. The sampling pattern we consider here is defined by

$$\Psi = \bigcup_{p=1}^{P} \left\{\mathcal{LAT}(T) + \underline{x}_p\right\} \quad \underline{x}_p \in \mathbb{R}^D \tag{13}$$

This sampling pattern is commonly referred to as a *recurrent sampling pattern*, see e.g.[2]. A 2D example is presented in Figure 6. The solid circles, in Figure 6, represent the points of $\mathcal{LAT}(T)$ and the hollow circles the additional points. Note that the pattern of the added samples in each shifted unit cell of $\mathcal{LAT}(T)$ is identical. The union of these sets is a recurrent sampling pattern, Ψ. A specific example of this situation arises when one utilizes multiple identical digital cameras on the same scene.

In the one dimensional case (see e.g. [4]) the *number* of distinct points added in each sampling period (unit cell) of $\mathcal{LAT}(T)$ determines the bandwidth of reconstructible signals. The corresponding multi dimensional case is more complex as we show below. Let $\underline{c}_l = 2\pi T^{-T}\underline{k}_l \in \mathcal{LAT}\left(2\pi T^{-T}\right)$ where $\{\underline{k}_l\}_{l=1}^{L} = \mathcal{SR}\left(R^T\right)$ and $L = |\det(R)|$. Then

it can be shown that

$$\mathcal{UC}\left(2\pi T_Q^{-T}\right) = \bigcup_{l=1}^{L}\left\{\mathcal{UC}\left(2\pi T^{-T}\right) + \underline{c}_l\right\} \tag{14}$$

Note that a similar construction has been demonstrated in Figure 5 (see Remark 2).

Consider next a bandlimited signal $f_c(\underline{x})$ such that

$$\text{support}\left(\widehat{f}_c(\underline{\omega})\right) \subseteq \mathcal{UC}\left(2\pi T_Q^{-T}\right) = \bigcup_{l=1}^{L}\left\{\mathcal{UC}\left(2\pi T^{-T}\right) + \underline{c}_l\right\} \tag{15}$$

Thus $\mathcal{LAT}(T_Q)$ is a 'Nyquist lattice' for this signal.

In the sequel, we make extensive use of the Generalized Sampling Expansions (GSE) results (see [13], [1] and [6]). For the benefit of the reader we formally restate the most general form of this result below:

Theorem 2 *Let $f_c(\underline{x})$, T_Q and T be as in (12) and (15). Suppose $f_c(\underline{x})$ is passed through a bank of L filters $\left\{\widehat{h}_p(\underline{\omega})\right\}_{p=1}^{L}$ to generate the signals $g_p(\underline{x})$. Namely, $\widehat{g}_p(\underline{\omega}) = \widehat{h}_p(\underline{\omega})\,\widehat{f}_c(\underline{\omega})$. Then, a necessary and sufficient condition that $f_c(\underline{x})$ can be reconstructed from $\{g_p(T\underline{n})\}_{p=1}^{L}$ is that the equation*

$$\begin{bmatrix} \widehat{h}_1(\underline{\omega}+\underline{c}_1) & \cdots & \widehat{h}_P(\underline{\omega}+\underline{c}_1) \\ \vdots & \ddots & \vdots \\ \widehat{h}_1(\underline{\omega}+\underline{c}_L) & \cdots & \widehat{h}_P(\underline{\omega}+\underline{c}_L) \end{bmatrix} \begin{bmatrix} \Phi_1(\underline{\omega},\underline{x}) \\ \Phi_2(\underline{\omega},\underline{x}) \\ \vdots \\ \Phi_P(\underline{\omega},\underline{x}) \end{bmatrix} = \begin{bmatrix} e^{j\underline{c}_1^T\underline{x}} \\ e^{j\underline{c}_2^T\underline{x}} \\ \vdots \\ e^{j\underline{c}_L^T\underline{x}} \end{bmatrix} \tag{16}$$

has a solution for all $\underline{x}$ and every $\underline{\omega} \in \mathcal{UC}\left(2\pi T^{-T}\right)$. Under these conditions, the reconstruction given by

$$f_c(\underline{x}) = \sum_{p=1}^{P}\sum_{\underline{n}\in\mathbb{Z}^D} g_p(T\underline{n})\,\varphi_p(\underline{x}-T\underline{n}) \tag{17}$$

where

$$\varphi_p(\underline{x}) = \frac{|\det(T)|}{(2\pi)^D}\int_{\mathcal{UC}(2\pi T^{-T})} \Phi_p(\underline{\omega},\underline{x})\,e^{j\underline{\omega}^T\underline{x}}d\underline{\omega} \tag{18}$$

and Φ_p are solution of (16).

Proof. See [6]. ■

We now return to recurrent sampling such that $f_c(\underline{x})$ is sampled on Ψ (see (13)). This problem can be reformulated as a special case of the GSE described in Theorem 2. Choosing $\widehat{h}_p(\underline{\omega}) = e^{j\underline{\omega}^T\underline{x}_p}$ we get $g_p(\underline{x}) = f_c\left(\underline{x}+\underline{x}_p\right)$ and sampling each on $\mathcal{LAT}(T)$ results in the same data as by the recurrent sampling. We can now readily apply Theorem 2. Specifically, we have for the case of interest here that

$$\begin{aligned} \begin{bmatrix} \widehat{h}_1(\underline{\omega}+\underline{c}_1) & \cdots & \widehat{h}_P(\underline{\omega}+\underline{c}_1) \\ \vdots & \ddots & \vdots \\ \widehat{h}_1(\underline{\omega}+\underline{c}_L) & \cdots & \widehat{h}_P(\underline{\omega}+\underline{c}_L) \end{bmatrix} &= H\cdot diag\left\{e^{j\underline{\omega}^T\underline{x}_p}\right\} \\ &\in \mathbb{C}^{L\times P} \end{aligned} \tag{19}$$

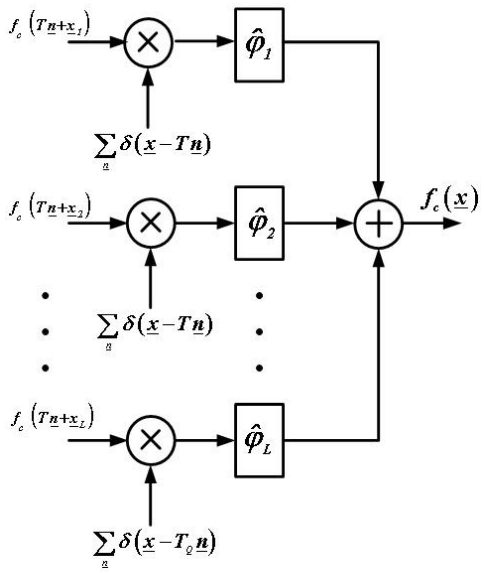

Figure 7: Reconstruction from recurrent nonuniform sampling.

where

$$H = \begin{bmatrix} e^{j\underline{c}_1^T\underline{x}_1} & e^{j\underline{c}_1^T\underline{x}_2} & \dots & e^{j\underline{c}_1^T\underline{x}_P} \\ e^{j\underline{c}_2^T\underline{x}_1} & e^{j\underline{c}_2^T\underline{x}_2} & \dots & e^{j\underline{c}_2^T\underline{x}_P} \\ \vdots & \vdots & \ddots & \vdots \\ e^{j\underline{c}_L^T\underline{x}_1} & e^{j\underline{c}_L^T\underline{x}_2} & \dots & e^{j\underline{c}_L^T\underline{x}_P} \end{bmatrix} \tag{20}$$

and (16) has a solution if H has *full row rank* (see [6]). A necessary condition for this to hold is clearly, that $L \leq P$. We assume, in the sequel, that $L = P$ and that the matrix H is non singular. Then, the reconstruction is carried out using (17) and (18).

Equation (17) can also be rewritten in an equivalent convolution form

$$f_c(\underline{x}) = \sum_{p=1}^{L} f_p(\underline{x}) * \varphi_p(\underline{x}) \tag{21}$$

where

$$f_p(\underline{x}) = \sum_{\underline{n}\in\mathbb{Z}^D} f_c\left(T\underline{n}+\underline{x}_p\right)\delta(\underline{x}-T\underline{n}) \tag{22}$$

This form of the result is depicted in Figure 7. We further illuminate this result below.

Let us denote $G = H^{-1}$ then from (16) and (19) we have

$$\Phi_p(\underline{\omega},\underline{x}) = e^{-j\underline{\omega}^T\underline{x}_p}\sum_{l=1}^{L} G_{p,l}e^{j\underline{c}_l^T\underline{x}}$$

and

$$\varphi_p(\underline{x}) = \frac{|\det(T)|}{(2\pi)^D}\int_{\mathcal{UC}(2\pi T^{-T})} e^{j\underline{\omega}^T(\underline{x}-\underline{x}_p)}d\underline{\omega}\sum_{l=1}^{L} G_{p,l}e^{j\underline{c}_l^T\underline{x}} \tag{23}$$

Then

$$\begin{aligned}
\widehat{\varphi}_p\left(\underline{\omega}\right) &= \int_{\mathbb{R}^D} \varphi_p\left(\underline{x}\right) e^{-j\underline{\omega}^T\underline{x}} d\underline{x} \\
&= \frac{\left|\det\left(T\right)\right|}{\left(2\pi\right)^D} \sum_{l=1}^{L} G_{p,l} \int_{\mathcal{UC}\left(2\pi T^{-T}\right)} \left[\int_{\mathbb{R}^D} e^{-j\left(\underline{\omega}-\underline{c}_l-\underline{\eta}\right)^T\underline{x}} d\underline{x}\right] e^{-j\underline{\eta}^T\underline{x}_p} d\underline{\eta} \\
&= \left|\det\left(T\right)\right| \sum_{l=1}^{L} G_{p,l} \int_{\mathcal{UC}\left(2\pi T^{-T}\right)} \delta\left(\underline{\omega}-\underline{c}_l-\underline{\eta}\right) e^{-j\underline{\eta}^T\underline{x}_p} d\underline{\eta} \\
&= \sum_{l=1}^{L} G_{p,l} e^{-j\left(\underline{\omega}-\underline{c}_l\right)^T\underline{x}_p} \widehat{h}_{LP}\left(\underline{\omega}-\underline{c}_l; \mathcal{UC}\left(2\pi T^{-T}\right)\right)
\end{aligned} \tag{24}$$

where we have used notation similar to the one in [4] for the ideal lowpass filter

$$\widehat{h}_{LP}\left(\underline{\omega}; \mathcal{UC}\left(2\pi T^{-T}\right)\right) = \begin{cases} \left|\det\left(T\right)\right| & \text{for} \quad \underline{\omega} \in \mathcal{UC}\left(2\pi T^{-T}\right) \\ 0 & \text{otherwise} \end{cases} \tag{25}$$

We see from (14), (16), (18) and (19) that $\widehat{\varphi}_p\left(\underline{\omega}\right) = 0$ for all $\underline{\omega} \notin \mathcal{UC}\left(2\pi T_Q^{-T}\right)$, namely, the filters $\widehat{\varphi}_p\left(\underline{\omega}\right)$ are bandlimited to the same bandwidth as the signal $f_c\left(\underline{x}\right)$. Thus, the reconstruction in Figure 7 is achieved via continuous filtering.

We will next utilize Theorem 1 to show how discrete filtering can be employed for this problem. To this end, we directly apply the result of Theorem 1 to each branch of Figure 7. This is illustrated in Figure 8 where, in this case, the discrete filters satisfy

$$\begin{aligned}
\widehat{\widehat{h}}_p\left(\underline{\omega}\right) &= \sum_{\underline{n}\in\mathbb{Z}^D} \widehat{\varphi}_p\left(\underline{\omega}+2\pi T_Q^{-T}\underline{n}\right) \\
&= \frac{1}{\left|\det\left(T_Q\right)\right|} \sum_{l=1}^{L} G_{p,l} e^{-j\left(\underline{\omega}-\underline{c}_l+2\pi T_Q^{-T}\underline{n}\right)^T\underline{x}_p} \\
&\qquad \widehat{h}_{LP}\left(\underline{\omega}-\underline{c}_l+2\pi T_Q^{-T}\underline{n}; \mathcal{P}\left(\Lambda^*\right)\right)
\end{aligned} \tag{26}$$

Thus, using Theorem 1, we have generated the samples on a Nyquist lattice. In many applications, this will be the desired end result. However, if the continuous signal is required, then one need only apply the low pass filter $\hat{h}_{LP}(\omega; \mathcal{UC}\left(2\pi T_Q^{-T}\right))$ as shown on the far right hand side of Figure 8.

5 Multi-dimensional Pth order nonuniform sampling.

In Section 4, the sampling used consisted of shifted versions of the *same* lattice. A further embellishment arises when one uses *distinct* lattices. A specific application would be the use of multiple cameras, each having a distinctive sampling pattern.

The combined sampling pattern in this case can be described as

$$\Psi = \bigcup_{p=1}^{P} \left\{\mathcal{LAT}\left(T_p\right) + \underline{x}_p\right\} \quad \underline{x}_p \in \mathbb{R}^D \tag{27}$$

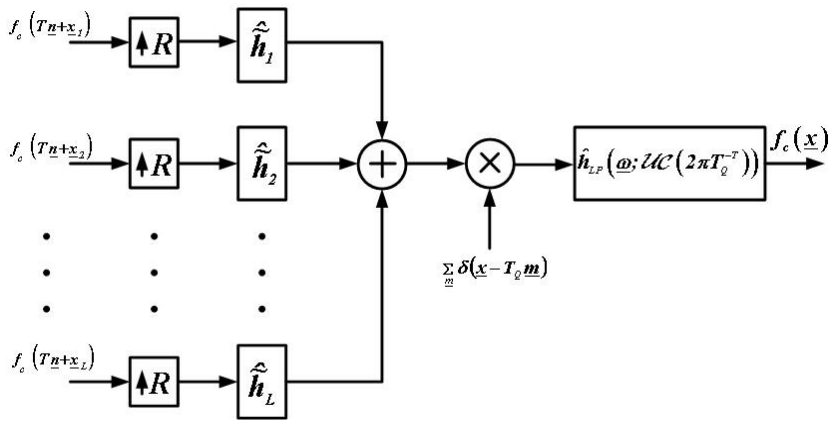

Figure 8: Discrete filter bank reconstruction from recurrent nonuniform sampling.

We again, assume that there exist a 'Nyquist' sampling lattice $\mathcal{LAT}\left(T_Q\right)$ and consider signals satisfying

$$\text{support}\left(\widehat{f}\left(\underline{\omega}\right)\right) \subseteq \mathcal{UC}\left(2\pi T_Q^{-T}\right) \tag{28}$$

We also assume that, for each T_p we have

$$\begin{aligned} T_p &= T_Q \widetilde{R} \widetilde{M}_p^{-1} \\ &= T_Q M_p^{-1} R_p \end{aligned} \tag{29}$$

with $\left|\det\left(M_p\right)\right| = \left|\det\left(\widetilde{M}_p\right)\right|$ for some nonsingular integral matrices $\widetilde{R}, \widetilde{M}_p$. Note that there is no loss of generality in assuming that $\widetilde{R}$ is common to all T_p since if it is not, we can always choose $\widetilde{R} = l.c.r.m\left(\widetilde{R}_p\right) = \widetilde{R}_p \widetilde{S}_p$ and replace the $\widetilde{M}_p$ by $\widetilde{M}_p \widetilde{S}_p$ maintaining the ratio and resulting in the form of (29).

We wish to reconstruct the signal $f\left(\underline{x}\right)$ from its samples on Ψ, namely, from the data set $\left\{f\left(\underline{x}\right) : \underline{x} \in \Psi\right\}$. Denoting

$$T = T_Q \widetilde{R} \tag{30}$$

we obtain from (29)

$$T_p = T \widetilde{M}_p^{-1} \tag{31}$$

Furthermore, let

$$\left\{\underline{\widetilde{m}}_{p,r}\right\}_{r=1}^{L_p} = \mathcal{SR}\left(\widetilde{M}_p\right) \tag{32}$$

where $L_p = \left|\det\left(\widetilde{M}_p\right)\right|$.

It can then be readily shown that

$$\Psi = \bigcup_{p=1}^{P} \bigcup_{r=1}^{L_p} \left\{\mathcal{LAT}\left(T\right) + \underline{x}_p + T_p \underline{\widetilde{m}}_{p,r}\right\} \tag{33}$$

Once put in this form, we can see that this problem is a special case of the recurrent sampling discussed in the previous section. Hence, denoting $L = \left|\det\left(\widetilde{R}\right)\right|$ we need to

have $L \leq \sum_{p=1}^{P} L_p$. We will assume $L = \sum_{p=1}^{P} L_p$, and, as in (15), that

$$\mathcal{UC}\left(2\pi T_Q^{-T}\right) = \bigcup_{q=1}^{P} \bigcup_{l=1}^{L_p} \left\{\mathcal{UC}\left(2\pi T^{-T}\right) + \underline{c}_{q,l}\right\} \tag{34}$$

where $\underline{c}_{q,l} = 2\pi T^{-T} \underline{\widetilde{n}}_{q,l}$ and $\bigcup_{q=1}^{P} \left\{\underline{\widetilde{n}}_{q,l}\right\}_{l=1}^{L_p} = \mathcal{SR}\left(\widetilde{R}^T\right)$ (The two indexed enumeration is adopted for notational convenience.)

Using (20) and (33) the resulting matrix H will have the form

$$H = \begin{bmatrix} H^{1,1} & \cdots & H^{1,P} \\ \vdots & \ddots & \vdots \\ H^{P,1} & \cdots & H^{P,P} \end{bmatrix} \tag{35}$$

where the (q,p)th block is

$$H^{q,p} = \begin{bmatrix} e^{j\underline{c}_{q,1}^T\left(\underline{x}_p + T_p\underline{\widetilde{m}}_{p,1}\right)} & e^{j\underline{c}_{q,1}^T\left(\underline{x}_p + T_p\underline{\widetilde{m}}_{p,2}\right)} & \cdots & e^{j\underline{c}_{q,1}^T\left(\underline{x}_p + T_p\underline{\widetilde{m}}_{p,L_p}\right)} \\ e^{j\underline{c}_{q,2}^T\left(\underline{x}_p + T_p\underline{\widetilde{m}}_{p,1}\right)} & e^{j\underline{c}_{q,2}^T\left(\underline{x}_p + T_p\underline{\widetilde{m}}_{p,2}\right)} & \cdots & e^{j\underline{c}_{q,2}^T\left(\underline{x}_p + T_p\underline{\widetilde{m}}_{p,L_p}\right)} \\ \vdots & \vdots & \ddots & \vdots \\ e^{j\underline{c}_{q,L_q}^T\left(\underline{x}_p + T_p\underline{\widetilde{m}}_{p,1}\right)} & e^{j\underline{c}_{q,L_q}^T\left(\underline{x}_p + T_p\underline{\widetilde{m}}_{p,2}\right)} & \cdots & e^{j\underline{c}_{q,L_q}^T\left(\underline{x}_p + T_p\underline{\widetilde{m}}_{p,L_p}\right)} \end{bmatrix} \in \mathbb{C}^{L_q \times L_p} \tag{36}$$

Assuming H is invertible with $G = H^{-1}$, the reconstruction formula, using continuous filtering, can then be obtained as in (17)-(24), i.e.

$$f\left(\underline{x}\right) = \sum_{p=1}^{P} \sum_{r=1}^{L_p} \sum_{\underline{n} \in \mathbb{Z}^D} f\left(T\underline{n} + \underline{x}_p + T_p\underline{\widetilde{m}}_{p,r}\right) \varphi_{p,r}\left(\underline{x} - T\underline{n}\right) \tag{37}$$

where

$$\varphi_{p,r}\left(\underline{x}\right) = \frac{\left|\det\left(T\right)\right|}{\left(2\pi\right)^D} \int_{\mathcal{UC}\left(2\pi T^{-T}\right)} e^{j\underline{\omega}^T\left(\underline{x} - \underline{x}_p - T_p\underline{\widetilde{m}}_{p,r}\right)} d\underline{\omega} \sum_{q=1}^{P} \sum_{l=1}^{L_q} \left(G^{p,q}\right)_{r,l} e^{j\underline{c}_{q,l}^T\underline{x}} \tag{38}$$

The reconstruction formula (37) can be reformulated as (see Appendix C for details):

$$f\left(\underline{x}\right) = \sum_{p=1}^{P} \left[\sum_{l=1}^{L_p} \sum_{\underline{m} \in \mathbb{Z}^D} f\left(T_p\underline{m} + \underline{x}_p\right) e^{-j2\pi\underline{\widetilde{k}}_{p,l}^T \widetilde{M}_p^{-1}\underline{m}} h_{p,l}\left(\underline{x} - T_p\underline{m}\right) \right] \tag{39}$$

where

$$\widehat{h}_{p,l}\left(\underline{\omega}\right) = \frac{1}{\left|\det\left(M_p\right)\right|} \sum_{r=1}^{L_p} e^{j\left(\underline{\omega} - 2\pi T^{-T}\underline{\widetilde{k}}_{p,l}\right)^T T_p\underline{\widetilde{m}}_{p,r}} \widehat{\varphi}_{p,r}\left(\underline{\omega}\right) \tag{40}$$

In (39), for every p, in the square brackets we have exactly the configuration described in Figure 3. Indeed, as stated earlier, (39) is the motivation for the general configuration we considered in our Interpolation Identity.

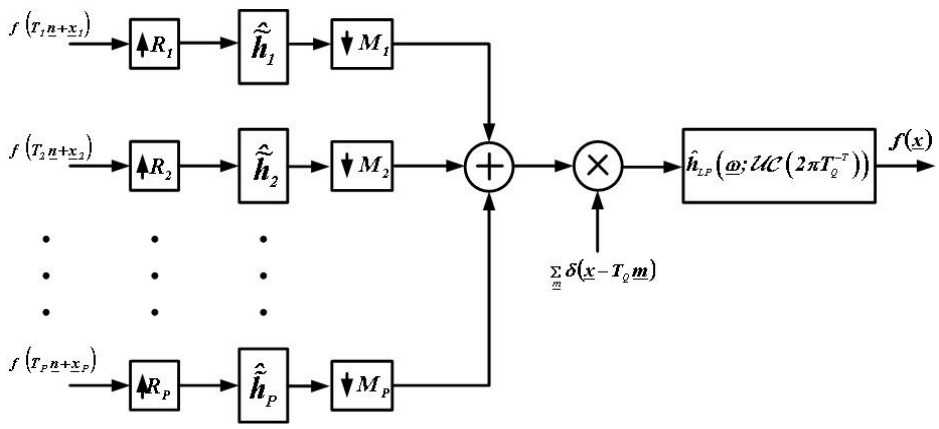

Figure 9: Reconstruction from Pth nonuniform sampling using a discrete filterbank.

Next we consider the case of discrete filtering. Using the Interpolation Identity of Theorem 1 the reconstruction can be carried out as depicted in Figure 9 where R_p and M_p are as in (29) and the filters $\widehat{\widehat{h}}_p$ are given by (see (11))

$$\widehat{\widehat{h}}_p(\underline{\omega}) = \frac{L_p}{|\det(T_Q)|} \sum_{\underline{n}\in\mathbb{Z}^D} \sum_{l=1}^{L_p} \widehat{h}_{p,l}\left(\underline{\omega} - 2\pi T_Q^{-T}\underline{k}_{p,l} + 2\pi T_Q^{-T} M_p^T \underline{n}\right) \tag{41}$$

where $\left\{\underline{k}_{p,l}\right\}_{l=1}^{L_p} = \mathcal{SR}\left(M_p^T\right)$. This leads to samples on a Nyquist lattice. Finally, the original signal can be reconstructed via a simple lowpass filter as shown on the far right hand side of Figure 9.

6 Conclusion

This paper has presented a generalized interpolation identity applicable to multi-dimensional signals. The identity establishes the equivalence of two multi-dimensional processing operations. The key point here is that one of these utilizes discrete processing operations and leads to the data being transferred to a "Nyquist lattice" from which the continuous signal, if required, can be readily reconstructed by a simple multi-dimensional low pass filter. We have also illustrated the application of the result to the special case of recurrent sampling. Beyond the cases discussed, we anticipate that the multi-dimensional result presented here will find wide spread application as already exemplified in [4] for the one dimensional case. In fact, the authors have been using the result presented here in a variety of multivariable reconstruction problems.

References

[1] K. F. Cheung. A multidimensional extension of Papoulis' generalized sampling expansion with application in minimum density sampling. *In: Advanced Topics in*

Shannon Sampling and Interpolation Theory., pages 86–119, Editor: R. J. Marks II 1993.

[2] Eric Dubois. Motion-compensated filtering of time-varying images. *Multidimensional Systems and Signal Processing*, 3:211–239, 1992.

[3] Robert J. Marks II (Editor). *Advanced Topics in Shannon Sampling and Interpolation Theory*. Springer Texts in Electrical Engineering. Springer-Verlag, 1993.

[4] Yonina C. Eldar and Alan V. Oppenheim. Filterbank reconstruction of bandlimited signals from nonuniform and generalized samples. *IEEE Transactions on Signal Processing*, 48(10):2864–2875, October 2000.

[5] Brian L. Evans. Designing commutative cascades of multidimensional upsamplers and downsamplers. *IEEE Signal Processing Letter*, 4(11):313–316, November 1997.

[6] A. Feuer. On the necessity of Papoulis result for multi-dimensional (GSE). *IEEE Signal Processing Letters*, 11(4):420–422, 2004.

[7] Arie Feuer and Graham C. Goodwin. *Sampling in Digital Signal Processing and Control*. Systems Control: Foundations Applications. Birhauser, 1996.

[8] Ramesh A. Gopinath and C. Sidney Burrus. On upsampling, downsampling, and rational sampling rate filter banks. *IEEE Transactions on Signal Processing*, 42(4):812–824, April 1994.

[9] Anil K. Jain. *Fundamentals of Digital Image Processing*. Prentice Hall Information and System Sciences Series. Prentice Hall, 1989.

[10] Jelena Kovacevic and Martin Vetterli. The commutativity of Up/Downsampling in two dimensions. *IEEE Transactions on Information Theory*, 37(3):695–698, May 1991.

[11] Cyrus Colton Macduffee. *Vectors and Matrices*. The Carus Mathematical Monographs. Mathematical Association of America, 1953.

[12] Morris Newman. *Integral Matrices*. Pure and Applied Mathematics. Academic Press, New York, 1972.

[13] A. Papoulis. Generalized sampling expansion. *IEEE Transactions on Circuits and Systems*, 24(11):652–654, November 1977.

[14] William K. Pratt. *Digital Image Processing*. John Wiley Sons, 3rd edition, 2001.

[15] P. P. Vaidyanathan. *Multirate Systems and Filter Banks*. Prentice Hall Signal Processing Series. Prentice Hall, 1993.

7 Appendix A: Proof of Lemma 1.

Proof. From the definitions of $\mathcal{SR}\left(M^T\right)$ and $\mathcal{SR}\left(\widetilde{M}^T\right)$ and (9), we have that for every $\underline{k} \in \mathcal{SR}\left(M^T\right)$ there exists a $\underline{\widetilde{k}} \in \mathcal{SR}\left(\widetilde{M}^T\right)$ such that $\underline{\widetilde{k}} = \rho\left(\underline{k}\right)$. Hence the mapping is onto. We use contradiction to establish the one to one property. Assume the converse of the result i.e., suppose that $\rho\left(\underline{k}_1\right) = \rho\left(\underline{k}_2\right)$ for some $\underline{k}_1 \neq \underline{k}_2 \in \mathcal{SR}\left(M^T\right)$. Then, by (9), for some $\underline{n}_1, \underline{n}_2 \in \mathbb{Z}^D$, we have

$$\widetilde{R}^T \underline{k}_1 - \widetilde{M}^T \underline{n}_1 = \widetilde{R}^T \underline{k}_2 - \widetilde{M}^T \underline{n}_2$$

or

$$\begin{aligned} \widetilde{R}^T\left(\underline{k}_1 - \underline{k}_2\right) &= \widetilde{M}^T\left(\underline{n}_1 - \underline{n}_2\right) \\ &= \underline{\ell} \in \mathbb{Z}^D \end{aligned} \tag{42}$$

Hence, $\underline{\ell} \in \left\{\widetilde{R}^T \underline{k} : \underline{k} \in \mathbb{Z}^D\right\} \cap \left\{\widetilde{M}^T \underline{n} : \underline{n} \in \mathbb{Z}^D\right\}$. However, using (3) we observe that

$$\begin{aligned} \left\{\widetilde{R}^T \underline{k} : \underline{k} \in \mathbb{Z}^D\right\} \cap \left\{\widetilde{M}^T \underline{n} : \underline{n} \in \mathbb{Z}^D\right\} &= \left\{\widetilde{R}^T M^T \underline{m} : \underline{m} \in \mathbb{Z}^D\right\} \\ &= \left\{\widetilde{M}^T R^T \underline{m} : \underline{m} \in \mathbb{Z}^D\right\} \end{aligned}$$

Thus, for some $\underline{m} \in \mathbb{Z}^D$, (42) implies that

$$\underline{\ell} = \widetilde{R}^T\left(\underline{k}_1 - \underline{k}_2\right) = \widetilde{R}^T M^T \underline{m}$$

namely,

$$\underline{k}_1 - \underline{k}_2 = M^T \underline{m} \Leftrightarrow \underline{k}_1 \equiv \underline{k}_2 \bmod \left(M^T\right)$$

However, since $\underline{k}_1, \underline{k}_2 \in \mathcal{SR}\left(M^T\right) \subset \mathcal{UC}\left(M^T\right)$ this necessarily implies that $\underline{k}_1 = \underline{k}_2$. This leads to a contradiction. Thus the claim is true. ■

8 Appendix B: Proof of Theorem 1.

Proof. To establish the identity we will derive expressions for the outputs of the configurations in Figures 3 and 4. We show that, for the same input, they are equal if (11) is satisfied. In Figure 3 we denote the input to the ℓth filter by $s_\ell\left(\underline{x}\right)$. Then

$$\begin{aligned} s_\ell\left(\underline{x}\right) &= f_c\left(\underline{x}\right) \sum_{\underline{n} \in \mathbb{Z}^D} e^{-j2\pi \underline{\widetilde{k}}_\ell^T \widetilde{M}^{-1} \underline{n}} \delta\left(\underline{x} - T\underline{n}\right) \\ &= f_c\left(\underline{x}\right) e^{-j2\pi \underline{\widetilde{k}}_\ell^T \widetilde{M}^{-1} T^{-1} \underline{x}} \sum_{\underline{n} \in \mathbb{Z}^D} \delta\left(\underline{x} - T\underline{n}\right) \\ & \qquad\qquad\qquad\qquad\qquad\qquad \ell = 1, ..., N \end{aligned} \tag{43}$$

The Fourier Transform (FT) of $s_\ell\left(\underline{x}\right)$ is

$$\widehat{s}_\ell\left(\underline{\omega}\right) = \frac{1}{\left|\det\left(T\right)\right|} \sum_{\underline{n} \in \mathbb{Z}^D} \widehat{f}_c\left(\underline{\omega} + 2\pi T^{-T} \widetilde{M}^{-T} \underline{\widetilde{k}}_\ell - 2\pi T^{-T} \underline{n}\right)$$

and hence

$$\widehat{y}_c = \frac{1}{|\det(T)|}\sum_{\ell=1}^{N}\widehat{h}_\ell(\underline{\omega})\sum_{\underline{n}\in\mathbb{Z}^D}\widehat{f}_c\left(\underline{\omega}+2\pi T^{-T}\widetilde{M}^{-T}\underline{k}_\ell-2\pi T^{-T}\underline{n}\right) \tag{44}$$

We next turn to the configuration in Figure 4. The Fourier transforms of $f(\underline{x}) = f_c(\underline{x})\sum_{\underline{n}\in\mathbb{Z}^D}\delta(\underline{x}-T\underline{n})$ is

$$\widehat{f}(\underline{\omega}) = \frac{1}{|\det(T)|}\sum_{\underline{n}\in\mathbb{Z}^D}\widehat{f}_c\left(\underline{\omega}-2\pi T^{-T}\underline{n}\right)$$

Since we use continuous frequency, the expansion operation by R to generate $f_e(\underline{x})$ does not affect the spectrum. Hence

$$\begin{aligned}\widehat{f}_e(\underline{\omega}) &= \widehat{f}(\underline{\omega})\\ &= \frac{1}{|\det(T)|}\sum_{\underline{n}\in\mathbb{Z}^D}\widehat{f}_c\left(\underline{\omega}-2\pi T^{-T}\underline{n}\right)\end{aligned} \tag{45}$$

However, since the signals $f_e(\underline{x})$ and $y_e(\underline{x})$ are sampled on the lattice $\mathcal{LAT}(TR^{-1})$, the filter $\widetilde{h}(\underline{x})$ has the property that its frequency response satisfies the following periodicity property

$$\widehat{\widetilde{h}}\left(\underline{\omega}+2\pi T^{-T}R^T\underline{m}\right) = \widehat{\widetilde{h}}(\underline{\omega}) \quad \text{for all} \quad \underline{m}\in\mathbb{Z}^D \tag{46}$$

Furthermore, it can be shown that the multi-dimensional decimation effect via M can be described in the frequency domain by

$$\widehat{y}_d(\underline{\omega}) = \frac{1}{N}\sum_{\ell=1}^{N}\widehat{y}_e\left(\underline{\omega}+2\pi T^{-T}R^TM^{-T}\underline{k}_\ell\right) \tag{47}$$

where we recall that $\underline{k}_\ell\in\mathcal{SR}\left(M^T\right) = \mathcal{UC}\left(M^T\right)\cap\mathbb{Z}^D$ and $N = |\det(M)| = \left|\det\left(\widetilde{M}\right)\right|$. Now, since $\widehat{y}_e(\underline{\omega}) = \widehat{\widetilde{h}}(\underline{\omega})\,\widehat{f}_e(\underline{\omega})$, we have

$$\widehat{y}_d(\underline{\omega}) = \frac{1}{N}\sum_{\ell=1}^{N}\widehat{\widetilde{h}}\left(\underline{\omega}+2\pi T^{-T}R^TM^{-T}\underline{k}_\ell\right)\widehat{f}_e\left(\underline{\omega}+2\pi T^{-T}R^TM^{-T}\underline{k}_\ell\right)$$

Then,

$$\begin{aligned}\widehat{y}_c(\underline{\omega}) &= \widehat{h}_{LP}(\underline{\omega})\,\widehat{y}_d(\underline{\omega})\\ &= \frac{1}{N}\widehat{h}_{LP}(\underline{\omega})\sum_{\ell=1}^{N}\widehat{\widetilde{h}}\left(\underline{\omega}+2\pi T^{-T}R^TM^{-T}\underline{k}_\ell\right)\widehat{f}_e\left(\underline{\omega}+2\pi T^{-T}R^TM^{-T}\underline{k}_\ell\right)\end{aligned}$$

Substituting into (45) we obtain

$$\begin{aligned}\widehat{y}_c(\underline{\omega}) = \frac{1}{N|\det(T)|}\widehat{h}_{LP}(\underline{\omega})\sum_{\ell=1}^{N}&\widehat{\widetilde{h}}\left(\underline{\omega}+2\pi T^{-T}R^TM^{-T}\underline{k}_\ell\right)\\ &\sum_{\underline{n}\in\mathbb{Z}^D}\widehat{f}_c\left(\underline{\omega}+2\pi T^{-T}R^TM^{-T}\underline{k}_\ell-2\pi T^{-T}\underline{n}\right)\end{aligned}$$

Using eqn. (3) and Lemma 1 the above expression can be rewritten as

$$\widehat{y}_c(\underline{\omega}) = \frac{1}{N|\det(T)|}\widehat{h}_{LP}(\underline{\omega})\sum_{\ell=1}^{N}\widehat{\widehat{h}}\left(\underline{\omega}+2\pi T^{-T}R^{T}M^{-T}\underline{k}_{\ell}\right) \sum_{\underline{n}\in\mathbb{Z}^D}\widehat{f}_c\left(\underline{\omega}+2\pi T^{-T}\widetilde{M}^{-T}\widetilde{R}^{T}\underline{k}_{\ell}-2\pi T^{-T}\underline{n}\right)$$

Applying Lemma 1 and (9) and (10) we obtain

$$\begin{aligned}\widehat{y}_c(\underline{\omega}) &= = \frac{1}{N|\det(T)|}\widehat{h}_{LP}(\underline{\omega})\sum_{\ell=1}^{N}\widehat{\widehat{h}}\left(\underline{\omega}+2\pi T^{-T}R^{T}M^{-T}\underline{k}_{\ell}\right) \\ &\qquad \sum_{\underline{n}\in\mathbb{Z}^D}\widehat{f}_c\left(\underline{\omega}+2\pi T^{-T}\widetilde{M}^{-T}\left(\widetilde{M}^{T}\underline{n}_{\ell}+\widetilde{\underline{k}}_{\ell}\right)-2\pi T^{-T}\underline{n}\right) \\ &= \frac{1}{N|\det(T)|}\widehat{h}_{LP}(\underline{\omega})\sum_{\ell=1}^{N}\widehat{\widehat{h}}\left(\underline{\omega}+2\pi T^{-T}R^{T}M^{-T}\underline{k}_{\ell}\right) \\ &\qquad \sum_{\underline{n}\in\mathbb{Z}^D}\widehat{f}_c\left(\underline{\omega}+2\pi T^{-T}\widetilde{M}^{-T}\widetilde{\underline{k}}_{\ell}-2\pi T^{-T}\underline{n}\right) \qquad (48)\end{aligned}$$

Comparing (44) to (48) we observe that the two outputs are equal if

$$\widehat{h}_{\ell}(\underline{\omega}) = \frac{1}{N}\widehat{h}_{LP}(\underline{\omega})\widehat{\widehat{h}}\left(\underline{\omega}+2\pi T^{-T}R^{T}M^{-T}\underline{k}_{\ell}\right)$$
$$\text{for every } \underline{\omega}\in\mathcal{UC}\left(2\pi T_Q^{-T}\right) \text{ and } \ell=1,2,...,N$$

or

$$\widehat{h}_{\ell}(\underline{\omega}) = \frac{1}{N}\widehat{h}_{LP}(\underline{\omega})\widehat{\widehat{h}}\left(\underline{\omega}+2\pi T_Q^{-T}\underline{k}_{\ell}\right)$$
$$\text{for every } \underline{\omega}\in\mathcal{UC}\left(2\pi T_Q^{-T}\right) \text{ and } \ell=1,2,...,N$$

Equation (11) follows. This completes the proof of the theorem. ■

9 Appendix C: Derivation of (39).

We begin by restating the reconstruction formula (38):

$$f(\underline{x}) = \sum_{p=1}^{P}\sum_{r=1}^{L_p}\sum_{\underline{n}\in\mathbb{Z}^D} f\left(T\underline{n}+\underline{x}_p+T_p\widetilde{\underline{m}}_{p,r}\right)\varphi_{p,r}(\underline{x}-T\underline{n})$$

which can also be rewritten as

$$f(\underline{x}) = \sum_{p=1}^{P}\sum_{r=1}^{L_p}\left[f\left(\underline{x}+\underline{x}_p+T_p\widetilde{\underline{m}}_{p,r}\right)\sum_{\underline{n}\in\mathbb{Z}^D}\delta(\underline{x}-T\underline{n})\right] * \varphi_{p,r}(\underline{x})$$

Then, in the frequency domain, we obtain

$$\widehat{f}\left(\underline{\omega}\right)=\frac{\left(2\pi\right)^{D}}{\left|\det\left(T\right)\right|}\sum_{\underline{n}\in\mathbb{Z}^{D}}\widehat{f}\left(\underline{\omega}-2\pi T^{-T}\underline{n}\right)\sum_{p=1}^{P}\sum_{r=1}^{L_{p}}e^{j\left(\underline{\omega}-2\pi T^{-T}\underline{n}\right)^{T}\left(\underline{x}_{p}+T_{p}\widetilde{\underline{m}}_{p,r}\right)}\widehat{\varphi}_{p,r}\left(\underline{\omega}\right)\qquad(49)$$

Let $\left\{\widetilde{\underline{k}}_{p,l}\right\}_{l=1}^{L_{p}}=\mathcal{SR}\left(\widetilde{M}_{p}^{T}\right)$ so that, for every $\underline{n}\in\mathbb{Z}^{D}$, we can write $\underline{n}=\widetilde{M}_{p}^{T}\underline{m}+\widetilde{\underline{k}}_{p,l}$. Then (49) can be rewritten as

$$\begin{aligned}\widehat{f}\left(\underline{\omega}\right)=&\frac{\left(2\pi\right)^{D}}{\left|\det\left(T\right)\right|}\sum_{p=1}^{P}\sum_{\underline{m}\in\mathbb{Z}^{D}}\sum_{l=1}^{L_{p}}\widehat{f}\left(\underline{\omega}-2\pi T^{-T}\widetilde{\underline{k}}_{p,l}-2\pi T_{p}^{-T}\underline{m}\right)\\&\sum_{r=1}^{L_{p}}e^{j\left(\underline{\omega}-2\pi T^{-T}\widetilde{\underline{k}}_{p,l}-2\pi T_{p}^{-T}\underline{m}\right)^{T}\underline{x}_{p}}e^{j\left(\underline{\omega}-2\pi T^{-T}\widetilde{\underline{k}}_{p,l}\right)^{T}T_{p}\widetilde{\underline{m}}_{p,r}}\widehat{\varphi}_{p,r}\left(\underline{\omega}\right)\end{aligned}$$

or

$$\begin{aligned}\widehat{f}\left(\underline{\omega}\right)=&\sum_{p=1}^{P}\sum_{l=1}^{L_{p}}\left(\left[\widehat{f}\left(\underline{\omega}-2\pi T^{-T}\widetilde{\underline{k}}_{p,l}\right)e^{j\left(\underline{\omega}-2\pi T^{-T}\widetilde{\underline{k}}_{p,l}\right)^{T}\underline{x}_{p}}\right]\right.\\&\left.*\frac{\left(2\pi\right)^{D}}{\left|\det\left(T_{p}\right)\right|}\sum_{\underline{m}\in\mathbb{Z}^{D}}\delta\left(\underline{\omega}-2\pi T_{p}^{-T}\underline{m}\right)\right)\\&\frac{1}{\left|\det\left(M_{p}\right)\right|}\sum_{r=1}^{L_{p}}e^{j\left(\underline{\omega}-2\pi T^{-T}\widetilde{\underline{k}}_{p,l}\right)^{T}T_{p}\widetilde{\underline{m}}_{p,r}}\widehat{\varphi}_{p,r}\left(\underline{\omega}\right)\qquad(50)\end{aligned}$$

Denoting

$$\widehat{h}_{p,l}\left(\underline{\omega}\right)=\frac{1}{\left|\det\left(M_{p}\right)\right|}\sum_{r=1}^{L_{p}}e^{j\left(\underline{\omega}-2\pi T^{-T}\widetilde{\underline{k}}_{p,l}\right)^{T}T_{p}\widetilde{\underline{m}}_{p,r}}\widehat{\varphi}_{p,r}\left(\underline{\omega}\right)$$

and applying the inverse Fourier transform to (50) and we obtain

$$\begin{aligned}f\left(\underline{x}\right)&=\sum_{p=1}^{P}\sum_{l=1}^{L_{p}}\sum_{\underline{m}\in\mathbb{Z}^{D}}\left[f\left(T_{p}\underline{m}+\underline{x}_{p}\right)e^{-j\left(2\pi T^{-T}\widetilde{\underline{k}}_{p,l}\right)^{T}T_{p}\underline{m}}\delta\left(\underline{x}-T_{p}\underline{m}\right)\right]*h_{p,l}\left(\underline{x}\right)\\&=\sum_{p=1}^{P}\sum_{l=1}^{L_{p}}\sum_{\underline{m}\in\mathbb{Z}^{D}}\left[f\left(T_{p}\underline{m}+\underline{x}_{p}\right)e^{-j2\pi\widetilde{\underline{k}}_{p,l}^{T}\widetilde{M}_{p}^{-1}\underline{m}}\delta\left(\underline{x}-T_{p}\underline{m}\right)\right]*h_{p,l}\left(\underline{x}\right)\end{aligned}$$

where we have used (31). The result (39) then follows.